Journal of Applied Polymer Science

# Dielectric features of two grades of bi-oriented isotactic polypropylene

**Abdelkader Kahouli,[1,2] Olivier Gallot-Lavallée,[1,2] Pacal Rain,[1,2] Olivier Lesaint,[1,2] Christophe Guillermin,[3] Jean-Marc Lupin[3]**

[1]Univ. Grenoble Alpes, G2Elab, F-38000 Grenoble, France
[2]CNRS, G2Elab, F-38000 Grenoble, France
[3]Rectiphase, Schneider Electric, Pringy F-74370, France
Correspondence to: O. Gallot-Lavallée (E-mail: olivier.gallot-lavallee@g2elab.grenoble-inp.fr)

**ABSTRACT:** The dielectric properties of two grades of bi-oriented isotactic polypropylene were studied with a variety of techniques: breakdown field measurements, dielectric spectroscopy, thermally stimulated depolarization currents (*I*s), and direct-current (dc) conduction *I* values. Standard polypropylene (STPP) and high-crystallinity polypropylene (HCPP) films were investigated. Measurements were carried out over a wide temperature range (−150°C/+125°C). The breakdown fields in both materials showed a very small difference. On the other hand, the dielectric losses and dc conduction *I* values were significantly lower in HCPP. Both materials showed a decrease in the dielectric loss versus temperature in the range 20–90°C; this is favorable for application in alternating-current power capacitors. The analysis of the dc *I* value allowed us to find evidence of two main conduction mechanisms: (1) below 80°C in both materials, a hopping mechanism due to the motion of electrons occurred in the amorphous phase, and (2) above 80°C, ionic conduction occurred in HCPP, and hopping conduction occurred in STPP. © 2015 Wiley Periodicals, Inc. J. Appl. Polym. Sci. **2015**, *132*, 42224.

**KEYWORDS:** applications; dielectric properties; structure; property relations

Received 1 December 2014; accepted 12 March 2015
**DOI: 10.1002/app.42224**

## INTRODUCTION

Semicrystalline polypropylene (PP) is a dielectric commonly used for power capacitor applications. Although it is known that the temperature, field, and frequency can greatly influence the electrical properties of this polymer, their influence on the conduction of the polymer is still not clear.[1]

Bi-oriented isotactic polypropylene (BOiPP) is one of the materials most frequently studied, and various mechanisms have been proposed to explain its behavior under alternating-current (ac) and direct-current (dc) conditions. The material structure, including its degree of crystallinity, constitutes parameters that may have an influence on the dielectric properties. In ref. 2, a study was carried out with the objective of proving the relationship between the structure of the film and its dielectric properties. Two main relaxation mechanisms were evidenced in addition to an increase in the crystallinity with film thickness, which correlated to an increase in the dielectric loss.

The objective of this study was to carry out a comparison of the properties of two PP film grades: a standard polypropylene (STPP) film identical to that studied ref. 2 and a high-crystallinity polypropylene (HCPP). This comparison was based on various phenomena and parameters:

1. The structural differences between STPP and HCPP first evidenced by an X-ray analysis.
2. Breakdown field measured under dc voltage.
3. Relaxation mechanisms evidenced by dielectric spectroscopy (DS) and thermally stimulated depolarization currents (TSDCs).
4. dc conduction properties, as determined from polarization and depolarization currents (*I*s) recorded under a rectangular voltage wave.

## EXPERIMENTAL

### Sample Properties

The studied BOiPP had a thickness of 11.8 $\mu$m. The starter process provided film samples stretched successively in two directions: the machine direction (MD) and then the transverse direction (TD). A Tenter process was used to build these films, with a typical stretching zone of 160°C/12 m and a thermosetting zone of 175°C/9 m. Two BOiPP materials with two crystallinity ratios were selected: STPP with a crystallinity ratio of about 46% and HCPP with a crystallinity ratio of about 53%. The latter had more catalyst and a second additional type of antioxidant. The crystallinity ratios were determined by differential scanning calorimetry (DSC). Their glass-transition

temperature ($T_g$) was around 0°C. The general properties of these samples are summarized in Table I.

### Sample Conditioning

Samples were received already metallized by an industrial process only on one side with aluminum (thickness ≈ 10 nm). For the DS, TSDC, and dc conduction measurements, the samples were additionally metallized on both sides by the evaporation of a silver layer, 30 nm in thickness, as in ref. 2. This was also done on the side already metallized to reduce the metallization surface resistance and favor the connection with the measurement system. The samples were then placed between massive flat electrodes and annealed at annealing temperature ($T_a$) = 120°C for 2 h under nitrogen in short-circuit conditions to erase the previous sample history (mechanical constraints, space charges, etc.). Then, they were slowly cooled to room temperature. This protocol ensured a rather good reproducibility of measurements. Breakdown measurements were carried out with the initial films and without additional metallization.

### *I* Response to dc Voltage

The *I*–time and *I*–voltage characteristics of the samples were measured with an electrometer (Keithley 6517 A). The temperature range was from 60 to 120°C and the electric field ranged from 0 to 85 V/μm. All of these measurements were done under inert gas ($N_2$). In the first experiments, an earthed guard ring surrounding the effective *I* measurement electrode [electrode area ($S$) = 3.14 $cm^2$] was implemented to prevent the influence of any surface *I* (electrode–guard ring distance = 2 mm). The use of the guard rings was subsequently discontinued because identical results were obtained in their absence.

### Thermostimulated Depolarization *I*

The thermoelectrical protocol used to identify the relaxation peaks is given in Figure 1. After preliminary annealing at $T_a$, the samples were first brought to a polarization temperature of 100°C. Then, a poling field of 60 V/μm was applied for a poling time of 10 min. Then, with the poling field still maintained, the sample was cooled down to a selected low temperature ($T_0$) to allow the polarization and space charge to freeze. The next steps were the removal of the field, short-circuiting of the sample, and maintenance of the sample at $T_0$ for a freezing time ($t_0$) of 3 min. In the final step, the sample was heated at a linear heating rate ($H_r$; °C/s) to measure the thermostimulated depolarization *I* generated versus temperature.

**Table I.** General Properties of the 11.8-μm BOiPP Films

| Characteristic | STPP | HCPP |
|---|---|---|
| Density (g/$cm^3$): ASTM D 792 | 0.905 | 0.905 |
| Crystallinity (%): DSC | 46 | 53 |
| Melting points (°C): DSC | 167–169 | 169–171 |
| Tensile strength (MPa): ASTM D 882 | 130 (MD), 280 (TD) | 130 (MD), 280 (TD) |
| Glass-transition (°C): DS at 70 Hz | −2 | 18 |

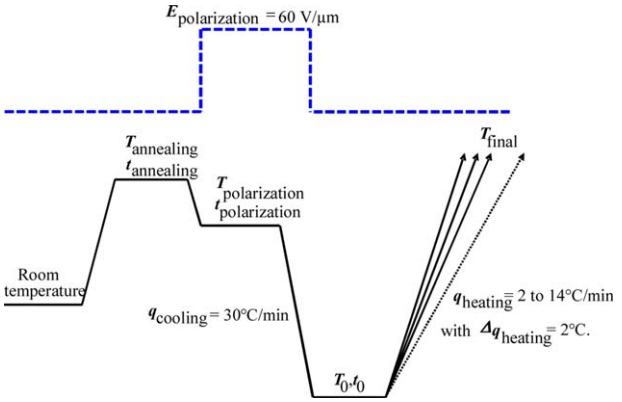


**Figure 1.** Thermoelectrical protocol for the TSDC measurement. $E_{polarization}$, electric field of polarization; $T_{polarization}$, temperature of polarization; $\Delta q_{heating}$, step between different rate of heating; $q_{heating}$, rate of heating; $q_{cooling}$, rate of cooling; $t_{annealing}$, time for annealing; $T_{annealing}$, temperature of annealing; $t_{polarization}$, time for depolarization; $T_{final}$, final (or stop) temperature. [Color figure can be viewed in the online issue, which is available at wileyonlinelibrary.com.]

### Breakdown Measurements

The film samples were placed between two plane electrodes with rounded edges and a good planarity and polished to a mirror finish. The film metallized side was placed onto a grounded electrode, 40 mm in diameter. The high-voltage electrode, 20 mm in diameter, was placed on the other side. To obtain reproducible measurements, we found it necessary to prevent the presence of dust by mounting the electrodes in a filtered-air facility and to repolish the electrodes between each breakdown test with a new sample. The dc voltage was raised at a linear rate (100 V/s) until breakdown occurred.

## RESULTS AND DISCUSSION

### Crystallinity Analyses

Figure 2 shows the X-ray diffraction patterns of STPP and HCPP obtained at room temperature. The diffraction peaks of HCPP

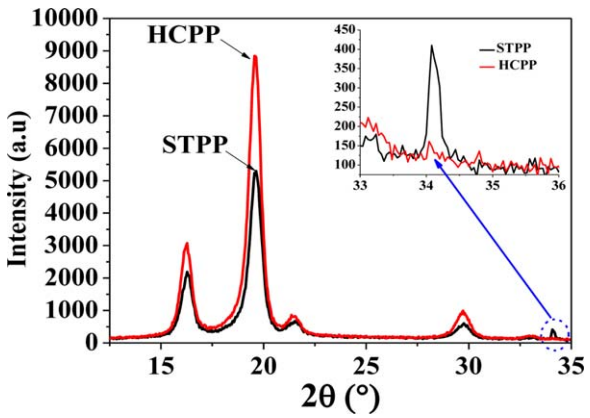


**Figure 2.** X-ray diffraction patterns of STPP and HCPP (11.8-μm films) obtained with Co Kα radiation (5000D Siemens). [Color figure can be viewed in the online issue, which is available at wileyonlinelibrary.com.]

had stronger intensities compared to those of STPP; this proved that HCPP contained more crystallites than STPP. This result was in agreement with other results obtained by DSC. We also observed that no displacement of diffraction peaks occurred with HCPP; this indicated the same crystal structure as STPP with the exception of the peak at $2\theta = 34.1°$. No more were observed with HCPP. Note that a measurement in transmission could clarify this apparent particularity. The X-ray profiles of STPP and HCPP coincided with typical diffraction patterns of the $\beta$-form crystallite ($\beta$ hexagonal), despite the effects of shifting on the emission peak because of the difference in X-ray (X) sources.[3]

### Dielectric Strength Measurement

Dielectric strength measurements of STPP versus temperature are shown in Figure 3. At each temperature, 16 samples were tested.

The data plotted in Figure 3 correspond to the averages of 16 measurements, and the error bars indicate the minimum and maximum values recorded. A slight decrease in the average breakdown field (ca. 10%) was observed when the temperature was raised up to 100°C. The breakdown field measured at 20°C with HCPP was quasi-identical to that with STPP, although the scatter of measurements was slightly reduced with HCPP.

### DS

Figure 4 (top) shows the measured dissipation factors (tan $\delta$ = relative losses factor ($\varepsilon''$)/relative permittivity ($\varepsilon'$) versus temperature at 70 Hz for STPP and HCPP. It was clear that the HCPP presented a lower tan $\delta$. We could also see the presence of two relaxation processes, already described in ref. 2, for STPP:

1. A $\beta^*$ relaxation in the temperature range −75 to −20°C produced a broad peak in tan $\delta$. This peak was attributed to the orientation of CH groups occurring in the amorphous phase.
2. A second $\alpha$-relaxation peak in the 0–20°C range, associated with the glass transition of the material, occurred in the mobile amorphous phase.

Figure 4 shows that in HCPP the $\alpha$ relaxation shifted to a higher temperature; this indicated a larger interchain interaction

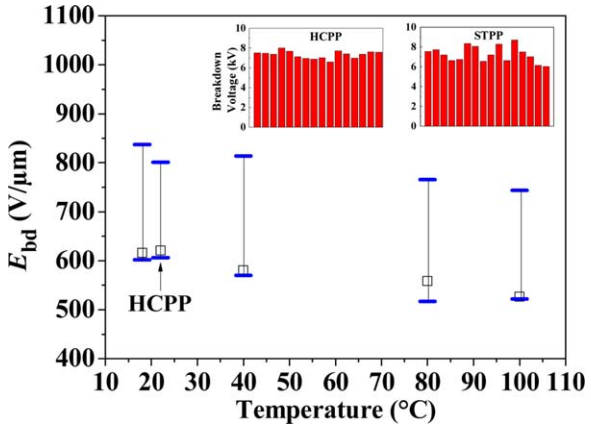


**Figure 3.** Dielectric strength versus temperature for an 11.8-µm STPP film with a dielectric strength at 20°C for an 11.8-$\mu$m HCPP film and typical scatter of the breakdown voltage measured at 20°C in both materials. $E_{bd}$, electric field of breakdown. [Color figure can be viewed in the online issue, which is available at wileyonlinelibrary.com.]

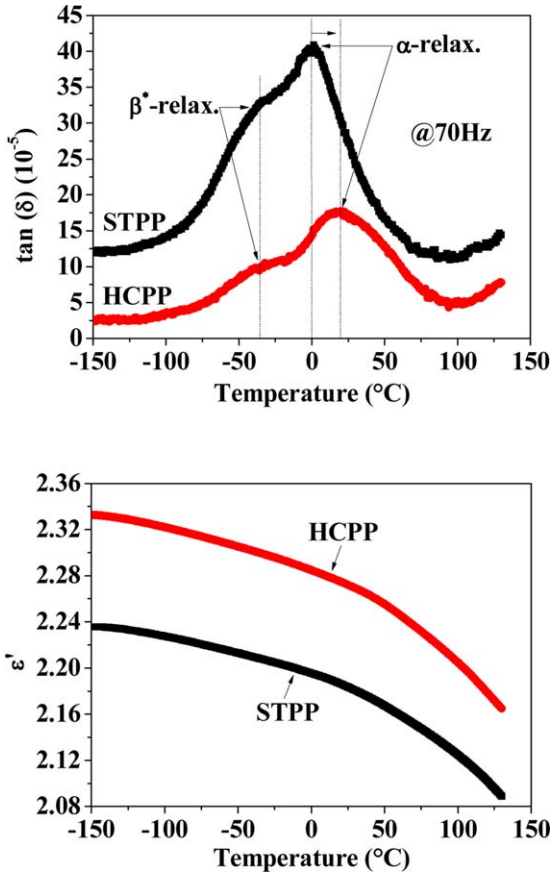


**Figure 4.** Variation of tan $\delta$ (top) and $\varepsilon'$ (bottom) versus temperature at 70 Hz for STPP and HCPP (11.8-µm films). [Color figure can be viewed in the online issue, which is available at wileyonlinelibrary.com.]

in the material. The $\beta^*$ relaxation associated with local motion remained unchanged. Consequently, an increase in the crystallinity affected the cooperative motion ($\alpha$ relaxation), whereas the local motion ($\beta^*$ relaxation) remained practically unchanged. In the same way, HCPP presented a higher real permittivity compared to STPP, as observed in Figure 4 (bottom). The permittivity decreased as the temperature increased; this was unlike what is usually seen in elastomers. In water, this trend is known and explained by micro-Brownian movement (Langevin–Debye).[4–6]

With regard to the dielectric properties, the main differences between materials could be summarized as follows: HCPP showed a significantly lower dielectric loss compared to STPP and a slightly higher dielectric constant. However, these variations could not be ascribed solely to the influence of crystallinity. The variations observed here (a decrease in the dielectric losses in HCPP) were even contradictory with those reported in ref. 2 when the crystallinity ratio of a single material varied under the influence of the elaboration process (in ref. 2, thicker films with a higher crystallinity ratio showed a higher dielectric losses). This led us to consider that the differences observed between HCPP and STPP were probably also due to the different chemical formulations used to produce these materials. The HCPP had more catalyst and a second additional type of antioxidant.

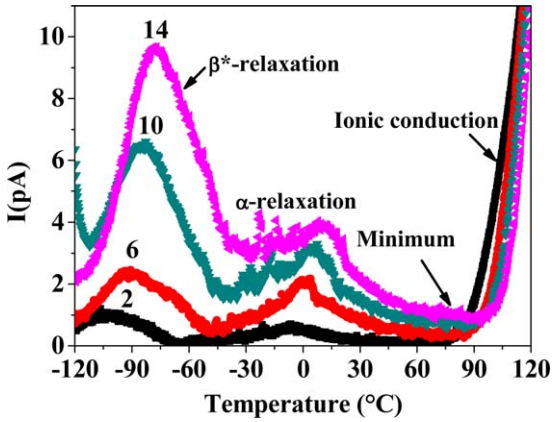


**Figure 5.** TSDC measurements of HCPP at different $H_r$ values from 2 to 14°C/min preceded by a poling electric field of 60 kV/mm (11.8-$\mu$m film). [Color figure can be viewed in the online issue, which is available at wileyonlinelibrary.com.]

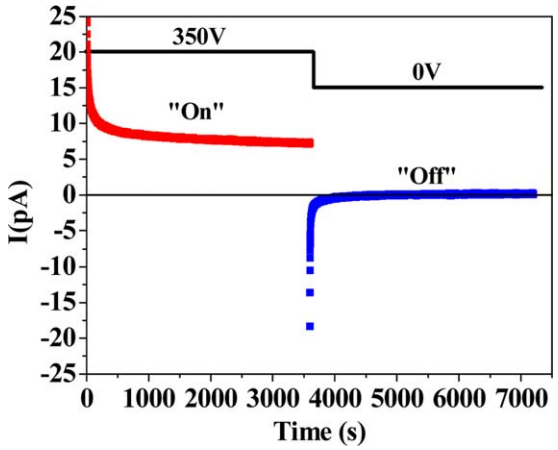


**Figure 6.** Polarization current ($I_p$) and depolarization current ($I_{dep}$) of STPP (11.8 $\mu$m) versus time at 350 V and 80°C. [Color figure can be viewed in the online issue, which is available at wileyonlinelibrary.com.]

### Thermally Stimulated *I* Values in HCPP

The results of TSDC measurements on HCPP are reported in the thermograms of Figure 5 (plots of TSDC *I* value vs temperature at different $H_r$ values).

Each plot showed two relaxation processes and a minimum TSDC spectrum. The first peak observed at −100°C for $H_r = 6$°C/min was associated with the $\beta^*$ relaxation. The second peak, which appeared at 0°C for $H_r = 6$°C/min, was attributed to $T_g$. These results were in good agreement with the results obtained by DS (Figure 4) and by dynamical mechanical analysis. The magnitudes $[I(T_M)]$ (where $T_m$ is Temperature corresponding to a any peak (alpha or beta)) of the peak intensities of the $\alpha$ and $\beta^*$ relaxations increased when $H_r$ was increased, and the peak positions $T_M$ shifted to a higher temperature. These results illustrate to what extent the relaxation processes involved here were thermally activated. Furthermore, these variations were related to each other in such a way that ln $I_M$ showed a linear dependence on $1/T_M$, with a slope equal to $-E_a/R$, as shown by eq. (1):[7]

$$\ln I_M = \frac{E_a}{R} \times \frac{1}{T_M} + a \qquad (1)$$

where R is the gas constant (molar gas constant) = 8,314 [J/(mol.K)], a is the arbitrary constant equivalent to ln(IM) at infinite temperature. $E_a$ is the barrier height of the trap states. From the fit of the TSDC data by eq. (1), the activation energy of the local relaxation process in the glass state of HCPP was equal to 0.34 eV. The same $E_a$ links to the local relaxation process were obtained for STPP.

### Conduction *I* Values

The classical way to measure the dc conduction *I* values consists of the application of a dc field and a wait for the stabilization of *I*. This occurs when the decreasing *I* component associated with polarization phenomena becomes much lower than the conduction *I* component. In very insulating materials, such as BOiPP, this may require a very long time, up to several days. An alternative faster method was used here. From measurements of transient *I* (Figure 6) with a rectangular voltage wave (1 h in duration), the sum of on plus off *I*s should represent the conduction *I*, provided that the *I* components associated with polarization are exactly symmetrical during the on and off phases.

The measurements (Figure 7, top, for STPP and Figure 7, bottom, for HCPP) showed large differences between the materials, with a conduction *I* that was about 1 decade lower in HCPP

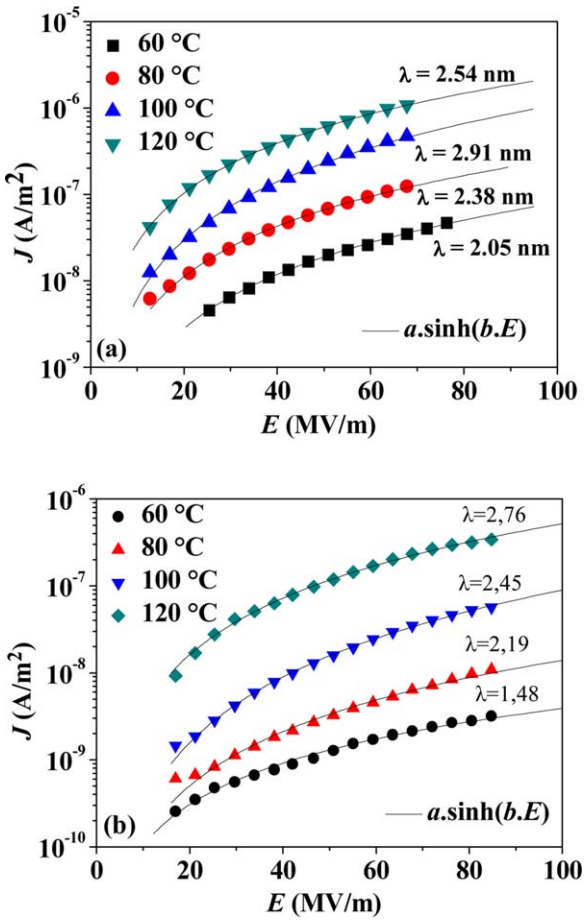


**Figure 7.** *J* versus log *E* for (top) STPP (11.8 μm) and (bottom) HCPP (11.8 μm) at various temperatures (60, 80, 100, and 120°C). b = arbitrary constant replacing = q.$\lambda$/(2.kb.T) cf equation (2); a = arbitrary constant replacing = 2.S.n.q.$\lambda$.v.exp(−Ea/(kb.T)) cf equation (2) [Color figure can be viewed in the online issue, which is available at wileyonlinelibrary.com.]

under identical conditions. On the basis of these measurements, we reviewed the different possible conduction mechanisms by fitting the data with the corresponding laws.

The hopping conduction mechanism provided the best fit of the measured *Is*:[8]

$$J(T,E)=2Snq\lambda v\exp\left(-\frac{E_a}{k_BT}\right)\sinh\left(\frac{q\lambda E}{2k_BT}\right) \quad (2)$$

where $J$ is the steady current density, $q$ is the carrier charge, $\lambda$ is the mean hopping distance of carrier, $n$ is the density of the carrier in the conduction band, $v$ is the frequency of the attempt of the carrier (electron/ion) to escape from the trap, $E$ is the applied electric field strength, $k_B$ is the Boltzmann constant, and $T$ is the absolute temperature.

The following mechanisms were, in turn. rejected: space charge limited current (SCLC), Pool–Frenkel, and Richardson–Schottky. In STPP, the activation energies required to fit the data (from 0.57 eV to 0.47 eV, as the field increased) indicated that conduction was governed by a hopping mechanism. The estimated $\lambda$ suggested that this electronic conduction occurred in the amorphous phase.[9,10]

In HCPP, two conduction regimes could be distinguished:

1. At low temperature of 80°C or below, a hopping mechanism due to multiple trapping and detrapping levels of electrons occurred, with activation energies of about 0.2–0.52 eV coming from shallow traps present in the amorphous phase and at the amorphous/crystal interface.[2,3,11,12]
2. At high temperatures of 80°C or above, ionic conduction occurred, with an activation energy of about 1.05 eV coming from the deep traps present in the crystalline phase.[13]

The different behaviors of the materials appeared to result mainly from conduction properties, which were characterized by a large difference in the measured dc *Is* (1 decade) and by different activation energies obtained by the fitting of the data with the hypothesis of a hopping conduction mechanism.

## CONCLUSIONS

Both grades of resin studied, HCPP and STPP, presented the following properties:

1. Similar dielectric strengths.
2. A conduction mechanism by hopping (at the explored temperatures of 60–120°C).
3. A dielectric $\beta$ relaxation mechanism.
4. A dielectric $\alpha$ relaxation mechanism with a slight increase in $T_g$ with crystallinity.

Quantitatively, there were some differences:

1. HCPP had ac and dc losses that were smaller and, conversely, a higher permittivity.
2. At high temperatures of 80°C or more, ionic conduction seemed to appear in HCPP instead of a conventional electronic conduction.

The physics behind these differences in behavior seemed to be the superposition of the effect of the degree of crystallinity[14] and the initial amount of catalyst and the difference in the quality and amount of antioxidant.

Finally, from a practical point of view (capacitors applications), the measurements carried out here suggest a better thermal stability with HCPP because of its reduced dielectric losses.

## REFERENCES


1. Foss, R. A.; Dannhauser, W. *J. Appl. Polym. Sci.* **1963**, *7*, 1015.
2. Kahouli, A.; Gallot-Lavallée, O.; Rain, P.; Lesaint, O.; Guillermin, C.; Lupin, J.-M. 2013 IEEE International Conference on Solid Dielectrics (ICSD), **2013**, pp. 1068–1071. http://ieeexplore.ieee.org.gaelnomade.ujf-grenoble.fr/xpls/abs_all.jsp?arnumber=6619684.
3. Brückner, S.; Meille, S. V.; Petraccone, V.; Pirozzi, B. *Prog. Polym. Sci.* **1991**, *16*, 361.
4. Debye, P. Polar Molecules; Chemical Catalog: New York, **1929**; p 172.
5. Von Hippel, A. R. Dielectrics and Waves; Chapman & Hall: New York, **1954**; p 174.
6. Kittel, C. Introduction to Solid State Physics; Wiley: New York, **1996**; p 610.
7. Ramos, J. J.; Correira, N. T.; Marques, R. T.; Collins, G. *Pharm. Res.* **2002**, *19*, 1879.
8. Das Gupta, D. K.; Joyner, K. *J. Phys. D* **1976**, *9*, 2041.
9. Karanja, P.; Nath, R. *J. Electrostatics* **1993**, *31*, 51.
10. Karanja, P.; Nath, R. *IEEE Trans. Dielectr. Electr. Insulation* **1994**, *1*, 213.
11. Arita, Y.; Shiratori, S. S.; Ikezaki, K. *J. Electrostatics* **2003**, *57*, 263.
12. Yamashita, T.; Ikezaki, K. *J. Electrostatics* **2005**, *63*, 559.
13. Kosaki, M.; Sugiyama, K.; Ieda, M. *J. Appl. Phys.* **1971**, *42*, 3388.
14. Ikezaki, K.; Kaneko, T.; Sakakibara, T. *Jpn. J. Appl. Phys.* **1981**, *20*, 609.